



ECM-targeting bacteria enhance chemotherapeutic drug efficacy by lowering IFP in tumor mouse models

Ji-Sun Kim^a, Jam-Eon Park^a, Seung-Hyeon Choi^a, Se Won Kang^a, Ju Huck Lee^a,
Jung-Sook Lee^a, Minsang Shin^b, Seung-Hwan Park^{a,*}

^a Biological Resource Center, Korea Research Institute of Bioscience and Biotechnology (KRIBB), Jeongup 56212, Republic of Korea

^b Department of Microbiology, School of Medicine, Kyungpook National University, 680 gukchaebosang-Ro, Jung-gu, Daegu 41944, Republic of Korea

ARTICLE INFO

Keywords:

Hyaluronidase
Extracellular matrix
Chemotherapeutic drug
Drug delivery
Bacterial cancer therapy

ABSTRACT

Bacterial cancer therapies aim to manipulate bacteria to effectively deploy therapeutic payloads to tumors. Attenuated bacteria alone often cannot eradicate solid tumors. Attenuated *Salmonella* can be engineered to deliver cytotoxic drugs to either trigger an immune response or increase antitumor efficacy when combined with chemotherapeutic drugs. However, the extracellular matrix (ECM) surrounding cancer cells forms a barrier that often limits the ability of chemotherapeutic and cytotoxic drugs to penetrate and eliminate tumors. To overcome this limitation, we developed a strategy to combine chemotherapy with an attenuated *Salmonella typhimurium* strain engineered to secrete HysA protein (from *Staphylococcus aureus*; Hyaluronidase, HAase) in tumors. The engineered *Salmonella* effectively degraded hyaluronan (HA), which is a major ECM constituent in tumors, and suppressed tumor growth in mouse models of pancreatic adenocarcinoma (ASPC-1) and breast cancer (4T1). Furthermore, it prolonged survival when combined with chemotherapeutic drugs (doxorubicin or gemcitabine). Upon bacterial colonization, the HAase-mediated ECM degradation decreased interstitial fluid pressure (IFP) in the tumor microenvironment. Additionally, HA degradation using HAase-expressing bacteria *in vivo* led to decreased binding to the receptor, CD44, expressed in tumors. This may modulate proliferation- and apoptosis-related signal pathways. Therefore, ECM-targeting bacteria can be used as a synergistic anticancer therapeutic agent to maximize chemotherapeutic drug delivery into highly invasive tumors.

1. Introduction

Bacterial genera such as *Clostridium*, *Listeria*, *Salmonella*, *Escherichia*, and *Bifidobacterium* [1–8] can grow within tumor microenvironments and suppress tumors. Recent studies have demonstrated that non-pathogenic, attenuated strains of *Salmonella typhimurium* that express cytolysin A (ClyA) can target and exert therapeutic effects in both subcutaneous and orthotopic xenograft models of human pancreatic cancers [9]. Bacterial cancer therapy (BCT) has been developed using engineered attenuated *S. typhimurium* strains, such as VNP20009 [10,11], A1-R [12,13], and ΔppGpp [14]. The VNP20009 strain, with *purI* and *msbB* deletions, has been used in clinical trials for patients with metastatic melanoma [11]. The A1-R strain, a leucine-arginine auxotroph, suppresses tumor growth in mouse models [15]. The ΔppGpp strain, with *recA* and *spoT* gene deletions, is defective in guanosine 5'-diphosphate synthesis and shows attenuated toxicity 100,000- to 1000,000-fold of its median lethal dose [9].

Bacteria can act as easily detectable “robot factories” that can specifically target tumors, actively penetrate tissues, and be controlled to induce cytotoxicity [16]. Other studies have suggested that bacteria may exert therapeutic effects by triggering inducible promoter gene expression [17], expressing cytotoxic drugs [6,17,18], imaging for visualization [19], genetic transfer [20], peptide cell-surface display [21], and in combination with anticancer agents [22]. Bacteria combined with chemotherapeutic drugs, such as triptolide, cyclophosphamide, gemcitabine, cisplatin, and doxorubicin [23–27], are promising BCT agents. They can act by suppressing tumor growth either directly or by inducing anticancer effects. Although these strategies have resulted in improved therapeutic effects, certain challenges remain. For example, chemotherapeutic drugs mainly diffuse *via* blood vessels in tumors owing to the higher interstitial fluid pressure (IFP) of the extracellular matrix (ECM) [28], thereby limiting the synergistic effects achievable with bacterial therapy [29]. This BCT approach is in stark contrast to conventional chemotherapy, wherein cytotoxic drugs indiscriminately affect normal

* Corresponding author.

E-mail address: biopark@kribb.re.kr (S.-H. Park).

<https://doi.org/10.1016/j.jconrel.2023.02.001>

Received 17 October 2022; Received in revised form 31 January 2023; Accepted 1 February 2023

Available online 7 February 2023

0168-3659/© 2023 The Authors. Published by Elsevier B.V. This is an open access article under the CC BY-NC-ND license (<http://creativecommons.org/licenses/by-nc-nd/4.0/>).

and cancer cells. When bacteria are administered *via* the tail vein, they transiently localize to organs composed of reticuloendothelial system (RES) such as liver and spleen [19]. Cytotoxic drugs are released only when the bacteria have cleared from the RES organs and accumulated in the targeted tumor tissues. This generally occurs 3 days after administration [30].

Hyaluronan (HA), also known as hyaluronic acid, is a major matrix molecule expressed in human malignancies [31]. It is significantly overexpressed in the ECM of pancreatic cancer (approximately 87%) and breast cancer (approximately 56%) [32], which results in an increased biophysical barrier that significantly increases IFP, compresses blood vessels, and hinders effective drug delivery [33,34]. Binding of HA to transmembrane receptor CD44 implicated in a variety of cellular events such as cell proliferation, migration, and invasion, which are necessary for inflammation and cancer progression [35,36]. Therefore, the development of CD44-targeted cancer therapy using anti-CD44 monoclonal antibodies, DNA vaccines, and nanoparticle-mediated delivery of CD44 siRNA has been attempted [37,38]. Hyaluronidase (HAase) is widely used in clinical applications, especially oncology, to facilitate the dispersion and absorption of interstitial fluid [39]. The HAase protein of *Staphylococcus aureus* ATCC 29213 shows higher enzyme activity than that derived from other strains [40]. HAase reduces the IFP in the tumor ECM, which is also an excellent facilitator of chemotherapy, as it activates the dispersion of the interstitial space *via* degrading HA in the ECM.

A previous study [41] demonstrated that the tumor-targeting attenuated *S. typhimurium*, which attached to the surface of HA-based microbeads *via* streptavidin–biotin conjugation, enhances chemotactic motion toward breast cancer 4T1 cells. Furthermore, an attenuated *S. typhimurium*-expressing HAase gene from *Streptomyces koganeensis* (bHs-ST) degrades HA of human PDAC tumors in mice, which enhances the antitumor effects of gemcitabine in only PANC-1 tumor xenografts [42]. However, the reason or mechanism by which HAase-expressing bacteria exhibit synergistic anticancer effects has not been elucidated. Our present study demonstrates that ECM-targeting bacteria can be used as a synergistic anticancer therapeutic agent to maximize chemotherapeutic drug delivery into highly invasive tumors. In the present study, we used an engineered ΔppGpp *S. typhimurium*, which is defective in guanosine 5'-diphosphate-3'-diphosphate (ppGpp). The engineered ΔppGpp has been demonstrated to have good biosafety and excellent anticancer efficacy in many reports [5,21,43–45]. We engineered bacteria to express and secrete a heterologous bacterial HAase to degrade the HA in the tumor ECM, thereby achieving the enhanced effects of combined chemotherapeutic drugs. To express HAase with optimal activity, we utilized the *hysA* gene from *S. aureus* ATCC 29213 and the *pelB* leader sequence fused upstream of *hysA* to precisely guide extracellular secretion. Here, HAase-expressing *Salmonella* degraded the HA in the ECM of tumors, decreased tumor IFP, disrupted the interaction between CD44 and HA, suppressed tumor proliferation, and induced apoptosis, which led to marked synergistic effects in anticancer efficacy of chemotherapeutic drugs. In the present study, we demonstrate a novel approach combining ECM-targeting bacteria with chemotherapeutic drugs for various tumors, such as pancreatic and breast cancers.

2. Materials and methods

2.1. Cells

Mouse breast cancer (4T1) and human pancreatic cancer (ASPC-1) cell lines were obtained from the ATCC (CRL-1682 and CRL-2539). Cells were grown in RPMI 1640 (ASPC-1) or high-glucose Dulbecco's Modified Eagle's Medium (4T1) (HyClone Lab, Inc., Logan, UT, USA) supplemented with 10% FBS and penicillin-streptomycin to a final concentration of 1%. They were cultured at 37 °C in a humidified atmosphere with 5% CO₂. Cells were counted using a hemocytometer (DHC-N01, inCYTO, Cheonan, Republic of Korea) and seeded into cell culture dishes

at a density of 1×10^6 cells per dish. The culture media were changed every 2 days until the cells reached 80% confluence.

2.2. Animal models

Five-to-six-week-old female BALB/c and male BALB/c athymic nu-/nu- mice (body weights: 20–25 g) were purchased from the Orient Company (Seongnam, Republic of Korea). All animal care, experiments, and euthanasia procedures were approved by the Committee of the Korea Research Institute of Bioscience and Biotechnology (approval number: KRIBB-AEC-20097, 20,172). Cell lines 4T1 and ASPC-1 were harvested at a density of 10^6 cells and 10^7 , respectively. They were suspended in 100 μL PBS before being subcutaneously injecting into the right thigh of each mouse. The subcutaneous tumor volume was assessed using a caliper every 3 days from day 3 to 25 for both cell lines. After the tumor volume reached approximately 120 mm³, PBS, bacterial strains (3×10^7 CFU), and chemotherapeutic drugs such as gemcitabine (5 mg/kg), doxorubicin (5 mg/kg), or paclitaxel (5 mg/kg) (see the treatment schedule below, 2.6) were injected intravenously in three experimental groups, respectively. Mice were anesthetized using 2% isoflurane to enable measurements of tumor volume or imaging to be conducted, or a mixture of ketamine (200 mg/kg) and xylazine (10 mg/kg) for implantation. Tumor volume (mm³) was calculated using the following formula: $(L \times H \times W)/2$, where L is the length, H is the height, and W is the width of the tumor in millimeters. Mice with a tumor volume ≥ 1000 mm³ were euthanized.

2.3. Bacterial strain and plasmid construction for HAase expression

The bacterial strain ΔppGpp *S. typhimurium* (SHJ2037; Δ*relA*::*Km*, Δ*spot*::*cm*) has been previously described [14]. Bioluminescence imaging was performed by transducing the whole luciferase operon of *Photobacterium luminescens* from *S. typhimurium*-Xen26 (Caliper Life Science, Hopkinton, USA) into SHJ2037 using P22HT *int*-mediated transduction (Table S1) [19].

To engineer HAase-expressing bacteria, the HAase gene (2640 base pairs) was amplified from *S. aureus* genomic DNA (*hysA* gene, ATCC 29213) [46] using the following primers: 5'-GCC ATG GCC ACA TAT AGA ATG AAG AAA TGG CAA AAA TTA TCC ACC -3' (forward primer) and 5'-CCG TTT AAA CTT ATT TAG TTA ATT CAA AGT GTA CGC CGG ATT C -3' (reverse primer). The amplicon was cut with the restriction enzymes *NcoI* and *PmeI* (NEB, Ipswich, Massachusetts, USA) to replace *Rluc8* at the same site in pBAD-*pelB*-*Rluc8* [47]. The resulting plasmid, pBAD-HAase (Fig. S1), was transferred into ΔppGpp *Salmonella* using the heat shock method (SL^{lux}/HAase). The resulting new strain was maintained in an ampicillin-containing medium and stored as a 20% glycerol stock at −80 °C.

2.4. Pre-treatment of *Salmonella* for *in vitro* and *in vivo* experiments

All bacterial strains were grown on LB agar plates containing the appropriate antibiotics. A single colony was selected, inoculated into LB media with antibiotics, and grown overnight at 37 °C and 200 rpm. The culture was diluted 50-fold using fresh media containing L-arabinose (final concentration 0.2%) to express the recombinant proteins and grown until the early stationary phase (OD₆₀₀ of 2.0–2.5). The culture was centrifuged at 4000 ×g for 10 min, washed with PBS, quantified using spectrophotometry, and diluted again with PBS. The fresh culture was adjusted to obtain the desired concentration of bacteria in an appropriate volume for the *in vitro* and *in vivo* experiments. *In vivo*, each cancer mouse model received 3×10^7 colony-forming units (CFU) suspended in 100 μL PBS. The bacterial count was calculated as follows: OD₆₀₀ of 1.0 = 0.8×10^9 CFU. To test whether the drug doses were toxic to bacteria, growth rates were measured for 10 h after administration of 0.1 mg/mL of each drug (gemcitabine, doxorubicin, and/or paclitaxel) in culture media. Since the weight of 5–6-week-old female BALB/c mice

used in the present study is approximately 20–25 g, the 0.1 mg/mL dose added to the culture medium is the mg/mL unit equivalent value of 5 mg/kg chemotherapeutic drug used to treat mice.

2.5. Qualitative and quantitation assays for HAase activity

A plate assay, using HA agar, was performed for the qualitative detection of HAase following a previously described method [40]. SL, SL^{HAase}, and SL^{lux/HAase} were streaked onto HA agar plates (with or without 0.2% L-arabinose) that were then incubated overnight at 37 °C. Each plate contained 2 M acetic acid to promote precipitation of undigested BSA-conjugated HA.

The quantitative turbidity assay for detecting HAase was performed following the enzymatic assay of HAase [48]. SL^{lux} or SL^{lux/HAase} (1 mL) was titrated to OD₆₀₀ of 1.0. The bacterial strains were washed with PBS, lysed by sonication using the Vibra-cell VCX 400 probe sonicator (Sonics & Materials Inc., Newtown, CT, USA), and harvested by centrifugation at 12,000 ×g for 10 min. The bacterial lysate was passed through a 0.22-μm filter and assayed for enzyme activity. To examine whether HAase expressed in SL^{lux/HAase} was secreted, we also performed the enzymatic assay of HAase in the culture supernatants and pellets. Samples were mixed with substrate solution containing 0.03% HA in 20 mM sodium phosphate buffer (pH 6.9) in a 1:1 ratio and the mixtures incubated for 45 min at 37 °C. The enzymatic reactions were stopped by adding 2.5 mL acidic albumin solution (79 mM acetic acid, 24 mM sodium acetate, and 0.1% BSA) and incubating for 10 mins at 25 °C. The enzyme activity was determined using a spectrophotometer (Shimadzu UV-1280). To calculate HAase activity, a standard curve of commercial HAase (from bovine testes; Sigma-Aldrich) dissolved in TSB was generated for every assay. For the *ex vivo* HAase assay, tumor tissues were analyzed at 0 and 25 days after injection, using a HAase activity enzyme-linked immunosorbent assay (ELISA) kit (K-6000; Echelon Bioscience, Inc., Salt Lake City, UT), according to the manufacturer's protocol.

2.6. Treatment schedule for chemotherapeutic drugs and bacterial administration

Anticancer treatments were performed using 4TI on day 15 or ASPC-1 on day 30 after tumor implantation. Tumor-bearing mice were divided into nine treatment groups: (i) PBS alone, (ii) gemcitabine alone, (iii) doxorubicin alone, (iv) paclitaxel alone, (v) *Salmonella* carrying an empty vector (SL^{lux}), (vi) HAase-expressing *Salmonella* with L-arabinose induction (SL^{lux/HAase}), (vii) HAase-expressing *Salmonella* with L-arabinose induction plus gemcitabine (5 mg/kg) (SL^{lux/HAase} + Gem), (viii) HAase-expressing *Salmonella* without L-arabinose induction plus doxorubicin (5 mg/kg) (SL^{lux/HAase(-)} + Doxo), (ix) HAase-expressing *Salmonella* with L-arabinose induction plus doxorubicin (5 mg/kg) (SL^{lux/HAase} + Doxo), and (x) HAase-expressing *Salmonella* with L-arabinose induction plus paclitaxel (5 mg/kg) (SL^{lux/HAase} + Pacl). Each of the anticancer drugs alone, or with bacterial groups, were administered at a dose of 5 mg/kg from days 5 to 26, every 3 days. The expression of HAase genes was induced by daily intraperitoneal administration of 0.12 g L-arabinose 3 days post injection (DPI).

2.7. Optical bioluminescence imaging

To image bacterial bioluminescence, the anesthetized mice were placed in a light-proof chamber within the IVIS imaging system (PerkinElmer, Waltham, MA, USA) at the Korea Basic Science Institute (Gwangju, Korea). It was equipped with a cooled charge-coupled device camera. Photons emitted from bioluminescent bacteria were collected and integrated over 1 min periods. Pseudocolor images indicating photon counts were overlaid on photographs of the mice using Living Image v.4.2 software.

2.8. Histopathological study

Mice tumors and livers were fixed in 3.7% paraformaldehyde overnight at room temperature (20–25 °C). The tissues were washed in PBS, transferred to 30% sucrose solution, and incubated overnight at 4 °C. Fixed tissues were embedded in optimal cutting temperature compound and stored at –80 °C. The paraffin-embedded tissue blocks were cut into 4 μm-thick longitudinal serial sections using a microtome (ThermoFisher, USA) and mounted onto glass slides for processing. Next, tissue sections were collected on aminopropyltriethoxysilane-coated slides and HRP-stained with the avidin-biotin conjugation method, using a Sequenza rack (Shandon, UK). For epitope retrieval, tissues were incubated for 30 mins at 125 °C with 10 mmol/L citrate buffer (pH 6.0) in a pressure cooker. Endogenous peroxidase activity was blocked by incubating samples in PBS (pH 7.4) containing 1.5% H₂O₂. For immunofluorescence and immunohistochemical staining, the slides were blocked with 5% BSA in PBS-T (containing 0.1% Triton X-100; Sigma-Aldrich, USA). The slides were incubated overnight at 4 °C with primary antibodies (Table S2). The sections were then washed three times with PBS or PBS-T and incubated with secondary antibodies (Table S2) for 3 h at room temperature. In case of TUNEL staining, the slide was labeled using MEBSTAIN Apoptosis TUNEL kit Direct (MBL, Japan) and counterstained with propidium iodide (0.5 μg/mL) and then with DAPI (1:10,000, Invitrogen). Next, the sections were mounted in ProLong Antifade Mountant (Invitrogen, USA) and examined under a FV1000D confocal laser scanning microscope for immunostaining and Mantra 2 Quantitative Pathology Workstation (Akoya Biosciences, USA) for HRP staining. The images were analyzed using FV10-ASW2.0 Viewer software (Olympus) and ImageScope v7.1.

2.9. Quantitative RT-PCR

Tumor tissues were collected and treated with RNeasy Protect Bacteria Reagent (Qiagen, Hilden, Germany) 6 h after L-arabinose induction at 3 DPI. Bacterial mRNA was obtained from the pellet using RNeasy Mini Kit (Qiagen) according to the recommended protocol. cDNA was generated from 1 μg total mRNA using oligo (dT) primers (Promega, USA) and ImProm-II Reverse Transcriptase (Promega). Quantitative RT-PCR was performed using SYBR green (Takara, Japan), and the following primers were used - *S. typhimurium* housekeeping gene (*aroC*): forward, 5'-TCG CCG ATC TCC ACG CCT TT-3', and reverse, 5'-GCG CGA AAG TGA CGG TGA TG-3'; and *hysA* primers: forward, 5'-GGT GCT TAT GGC GTT GTA CT-3', and reverse, 5'-CGT GAT AAA TCC ATC ATT TCA CC-3'. The reaction was carried out on CFX Connect machine (Bio-Rad) under the following conditions: 10 min at 95 °C, followed by 40 cycles at 95 °C for 15 s, 58 °C for 30 s, and 72 °C for 15 s. The amount of *hysA* mRNA was determined by comparison with that of the housekeeping gene *Salmonella aroC* (data expressed as the fold difference).

2.10. IFP measurement

Ozerdem et al. (2005) [49] described the reliable measurement of interstitial fluid pressure (IFP) in cancer tissues using a polyurethane transducer-tipped catheter (Millar Instruments, Houston, USA), and the unit for IFP value is cmH₂O. IFP was measured using the “wick-in-needle” probe technique [49] using a MicroTip catheter transducer (SPR; Millar Instruments, Houston, USA) with a 23.5-gauge wing-tipped needle. The transducer was interfaced with a PC using a pressure control unit (PCU-2000; Millar Instruments, Houston, USA). Data were converted using a USB analog-to-digital converter (DT9816; Data Translation). The needle was inserted into the tumors, and measurements taken every few millimeters along the entry path were averaged. The instrument was calibrated using a custom-built water column manometer.

2.11. Clinical chemistry parameters

On days 0 and 3, blood samples from all mice groups were obtained at the same time point following after the bacterial injections by heart puncture using heparinized syringes. To separate the sera, they were deposited in serum separator gel tubes (Microtainer, Becton-Dickinson, Franklin Park, NJ, USA) and centrifuged at $9300 \times g$ for 30 min at 4°C . The sera were immediately analyzed for biochemical parameters, such as aspartate aminotransferase and alanine aminotransferase activity. Additionally, concentrations of blood urea nitrogen, creatinine, C-reactive protein (CRP), and procalcitonin were determined using an automated analyzer (Hitachi Instruments, Tokyo, Japan) according to the manufacturer's instructions. Standard controls were run before each measurement, and the values obtained were within the expected ranges.

2.12. Western blot analysis

The tumors were removed 12 days after the bacterial injections with or without doxorubicin. Total proteins equal to $40\ \mu\text{g}$ were separated by electrophoresis and blotted. Protein content was standardized in homogenized tissue samples, and samples containing $100\ \mu\text{g}$ protein were subjected to SDS-PAGE using 8–12% linear gradient resolving gels. The proteins were transferred to nitrocellulose membranes (Bio-Rad, CA, USA), which were then probed using primary antibodies and incubated with a horseradish peroxidase (HRP)-conjugated secondary antibody (Table S2). Immunoreactive proteins were detected using Luminol reagent (Santa Cruz Biotechnology) and visualized using a Fujifilm image reader (LAS-3000).

2.13. FACS and ELISA analysis

The tumors ($n = 3/\text{group}$) were isolated from 4T1 tumor-bearing mice at 25 days after L-arabinose induction on 4 DPI. For FACS analysis, single-cell suspensions from 4T1 tumors were prepared by incubating removed tumor pieces in $2.0\ \text{mg/mL}$ collagenase D (Roche) and $50\ \mu\text{g/mL}$ DNase I (Roche) for 30 min at 37°C , followed by passing through a $40\ \mu\text{m}$ cell strainer. Samples were incubated with specific fluorochrome-labeled antibodies (Supplementary Table S2) at 4°C for 1 h. At least 100,000 events were analyzed using Attune™ NxT Flow Cytometer (ThermoFisher). Data were analyzed using Attune™ NxT v3.1.2 software. The analysis gate was set based on isotype plots. For ELISA analysis, protein lysates were collected from supernatant after multiple centrifugations. The expression levels of IL-1 β and TNF- α in the supernatants of the tumor tissue homogenates were detected by ELISA kits in accordance with the manufacturer's protocol (eBioscience).

2.14. Statistical analysis

Statistical analyses were performed using the GraphPad 8.0 software. Mann–Whitney U test was used to determine the statistical significance of the differences in primary tumor growth, quantitative analysis of HAase activity, mRNA expression, tumor IFP measurements, proliferation and apoptosis of tumor cells, and levels of inflammatory cytokines across groups. The Kruskal–Wallis test was performed to determine the differences in the clinical chemistry parameters. A P value < 0.05 was considered significant for all analyses. Survival analyses were performed using the Kaplan–Meier method and the log-rank test. All data are expressed as mean \pm standard deviation (SD).

3. Results

3.1. Tight regulation of HAase expression in attenuated *Salmonella* strains

To engineer HAase-expressing bacteria with active therapeutic effects in tumor tissues, we used the attenuated ΔppGpp *S. typhimurium*.

To express HAase with optimal activity, we utilized the *hysA* gene from *S. aureus* ATCC 29213. Before constructing the *hysA*-inducing vector system, it was also confirmed production, extracellular secretion, and HA degradation activity of HAase in the *S. aureus* (Fig. S1a). To construct an inducible vector system for ECM-degradable gene expression, we cloned *hysA* into the pBAD plasmid vector (Fig. S1b). Here, the *pelB* leader sequence was fused upstream of *hysA* to guide extracellular secretion. Expression of the plasmid (pBAD-*pelB*-*hysA*; pBAD-HAase) was induced only in the presence of L-arabinose (Fig. S1b). The plasmid pBAD-HAase was transformed into ΔppGpp *S. typhimurium* (SL^{HAase}) and ΔppGpp *S. typhimurium* harboring the luciferase operon ($\text{SL}^{\text{luc/HAase}}$). The growth of engineered bacteria ($\text{SL}^{\text{luc/HAase}}$) was not affected by HAase induction (Fig. S1c).

The plate assay performed to qualitatively examine the HAase activity in HAase-expressing bacteria (SL^{HAase} and $\text{SL}^{\text{luc/HAase}}$) displayed a clear zone around streaked colonies in the presence of HA (Fig. 1a). The bacterial signals were imaged using the IVIS imaging system. The turbidity assay quantitatively demonstrated that HAase activity in $\text{SL}^{\text{luc/HAase}}$ increased by approximately 37 units in the presence of L-arabinose (Fig. 1b) and HAase expressed in $\text{SL}^{\text{luc/HAase}}$ was secreted from bacteria (Fig. S2). These results indicated that HAase expression was tightly regulated by L-arabinose, and HAase was successfully secreted from the bacteria and that it subsequently degraded HA.

3.2. HAase-expressing bacteria degrade HA in the ECM of tumor tissues

HA regulates tumor growth and progression *in vivo* [50,51]. We confirmed HAase activity in 4T1 and ASPC-1 tumor tissues by HRP staining of biotinylated HA-binding protein (HABP) using immunofluorescence (Fig. 2a and b). Fig. 2b also shows that abundant bacteria were observed in the tumor tissues of *Salmonella*-injected mice, while no bacteria were observed in PBS-injected mice. The histological analysis revealed that the decrease of the HABP signal was observed only in the $\text{SL}^{\text{luc/HAase}}$ group, which was because the HAase expressed in the $\text{SL}^{\text{luc/HAase}}$ group degraded HA in the ECM of tumor tissues (Fig. 2a and b). Additionally, qRT-PCR of the excised ASPC-1 tumor tissue revealed that the HAase mRNA expression in tumors colonized by $\text{SL}^{\text{luc/HAase}}$ was 429-fold higher than that of a housekeeping gene (*aroC*) in the presence of L-arabinose. However, it was 95-fold higher in the absence of L-arabinose (Fig. 2c). These results showed that $\text{SL}^{\text{luc/HAase}}$ was tightly regulated in tumor tissues and expressed HAase also degraded HA in the ECM of tumor tissues.

3.3. Tumor IFP is reduced by HAase

HA in the ECM increases tumor IFP to inhibit the effectiveness of small molecule-based therapeutics. The systemic administration of enzymatic agents can ablate stromal HA from pancreatic and breast cancers, stabilize IFP and re-expand the microvasculature to induce functional perfusion [29]. To verify whether HAase released by the engineered bacteria reduced the IFP within the tumor ECM, we excised 4T1 and ASPC-1 tumor tissues after administrating the engineered bacteria (PBS, SL^{luc} , or $\text{SL}^{\text{luc/HAase}}$). On day 6 after surgery, tumor-bearing mice were divided into three groups: the negative control that received PBS (group 1), SL^{luc} carrying an empty vector (group 2), and $\text{SL}^{\text{luc/HAase}}$ with L-arabinose induction (group 3). It was observed that HAase-expressing bacteria significantly suppressed the tumor IFP cm-H₂O of the ECM ($P < 0.0001$) (Fig. 3a and b). These results indicated that the HAase expressed from the $\text{SL}^{\text{luc/HAase}}$ reduced the tumor IFP.

3.4. Tumor-suppressive effects of HAase-expressing *Salmonella* combined with chemotherapeutic drugs in tumor xenograft-bearing mice

HA, which is a major component of the ECM, is overexpressed in pancreatic and breast cancers [31]. To verify whether HAase-expressing bacteria suppress tumor growth by decreasing the IFP, we investigated

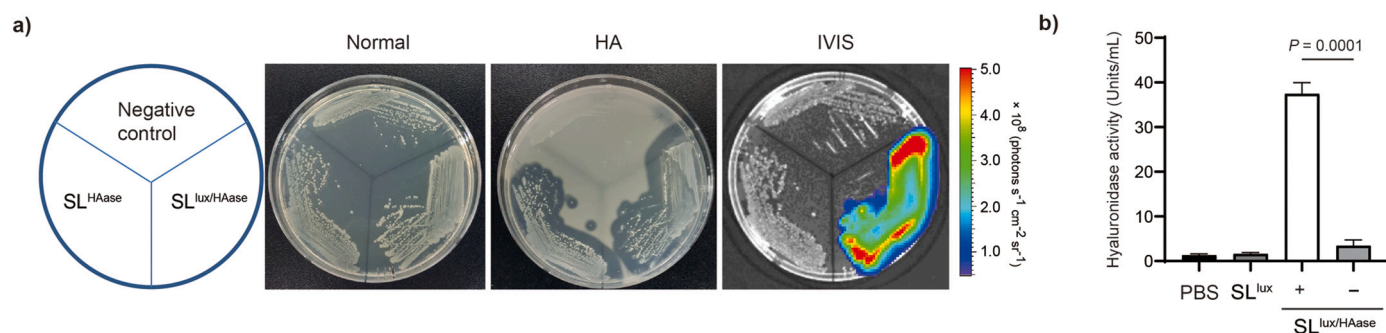


Fig. 1. Measurements of HAase activity in engineered HAase-expressing bacteria. pBAD-HAase plasmid was transformed into *S. typhimurium* (SL^{lux}). a) Regulation of transformed bacteria was performed with L-arabinose induction. Three bacterial groups were used (indicated left drawing). Left (Normal): SL (negative control), SL^{HAase}, or SL^{lux/HAase} were streaked on LB plate that was then incubated overnight at 37 °C. Center (HA): SL (negative control), SL^{HAase}, or SL^{lux/HAase} were grown on tryptic soy agar plate supplemented with hyaluronic acid and then treated with 2 M acetic acid the next day. The clear zone indicates hyaluronan breakdown. Right (IVIS): SL (negative control), SL^{HAase}, or SL^{lux/HAase} were grown on LB plate that was then incubated overnight at 37 °C. Bioluminescence was measured immediately using a cooled CCD camera. b) Quantitative analysis of HAase activity of the engineered bacteria. SL^{lux/HAase} were induced to express HAase treated with (+) or without (-) L-arabinose. Data are representative of three independent experiments. SL^{lux/HAase}, HAase-expressing *Salmonella* with L-arabinose induction.

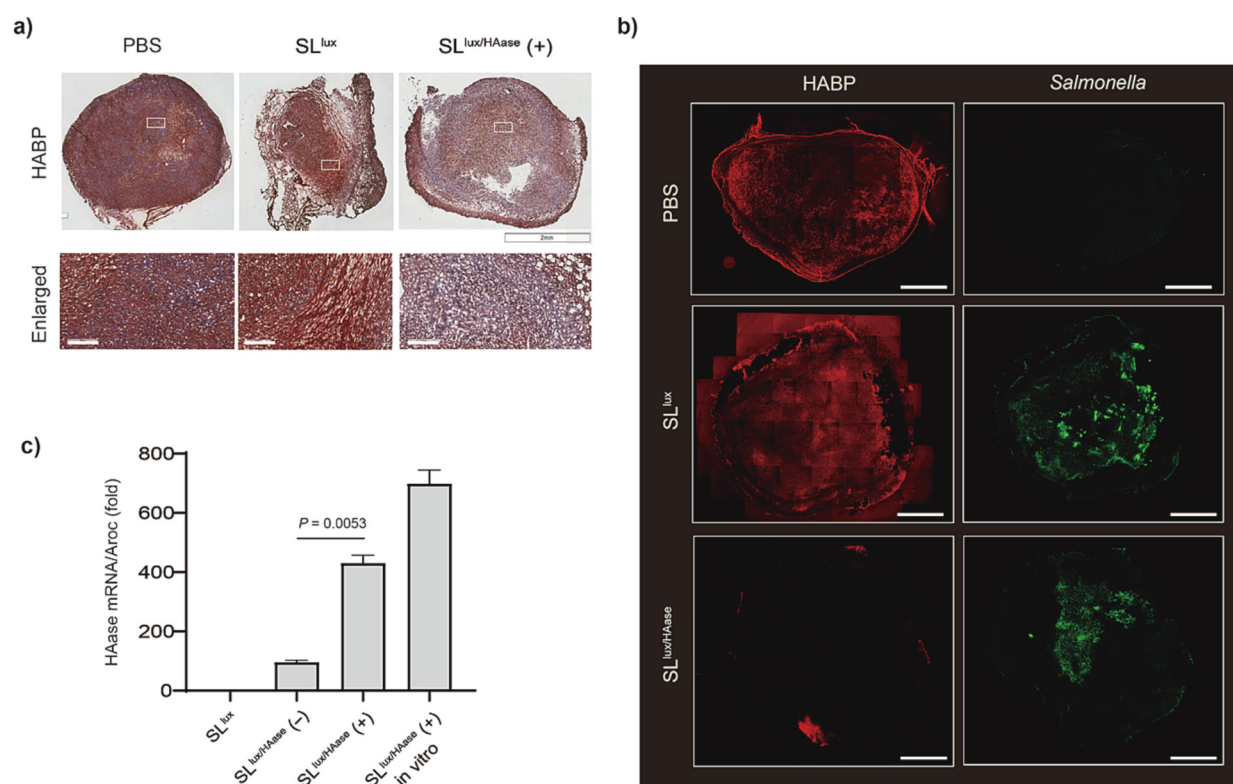


Fig. 2. In vivo hyaluronan degradation by HAase-expressing bacteria. BALB/c or BALB/c athymic nu-/nu- mice ($n = 8$ per group) received subcutaneous injections of 4T1 (1×10^6) or ASPC-1 (1×10^7) cells. When the tumor volumes reached approximately 150 mm^3 , the tumor-bearing mice were injected with PBS, SL^{lux}, or SL^{lux/HAase}, followed by intraperitoneal injections of L-arabinose at 4 days post infection (DPI). Immunohistological and immunofluorescence analyses ($n = 3$ per each), and total bacterial mRNA expression analyses ($n = 5$ per each) were performed after the excision of tumor grafts treated with *S. typhimurium*. a) Immunohistological analysis of the HABP detection in 4T1 tumor tissues from mice injected with PBS, SL^{lux} or SL^{lux/HAase} at 5 DPI. Scale bar = 2 mm and 200 μm (enlarged). b) Immunofluorescence staining with HABP (red) and anti-Salmonella antibody (green) in ASPC-1 tumor tissues from mice injected with PBS, SL^{lux}, or SL^{lux/HAase} at 5 DPI. The immunofluorescence images were generated by placing confocal images end-to-end. Scale bar = 2 mm. c) Total bacterial mRNA was extracted from ASPC-1 tumor tissues infected with SL^{lux} or SL^{lux/HAase} with (+) or without (-) L-arabinose induction (for 6 h at 4 DPI). mRNA from in vitro-cultured SL^{lux/HAase} (+) was used as the positive control. HAase mRNA was quantified using RT-PCR and the result normalized to that for the *aroC* house keeping gene. Data are expressed as the fold difference in expression. HABP, HA-binding protein; SL^{lux}, *Salmonella* carrying an empty vector; SL^{lux/HAase}, HAase-expressing *Salmonella* with L-arabinose induction. (For interpretation of the references to colour in this figure legend, the reader is referred to the web version of this article.)

the therapeutic effects in 4T1 and ASPC-1 tumor models. Furthermore, we explored the antitumor effects of engineered *Salmonella* (3×10^7 CFU) combined with chemotherapeutic drugs (5 mg/kg) (Figs. 4 and 5). As described in the 'Materials and methods' section, before treatment in mice, the growth rate of SL^{lux/HAase} was examined for 10 h after culture

media were treated with 0.1 mg/mL of chemotherapeutic drugs, demonstrating that the administration doses of chemotherapeutic drugs were not toxic to bacteria (Fig. S3). After treatment with PBS, engineered bacteria (SL^{lux} and SL^{lux/HAase}), a combination of SL^{lux/HAase} with doxorubicin (as a control) and a combination of SL^{lux/HAase} with

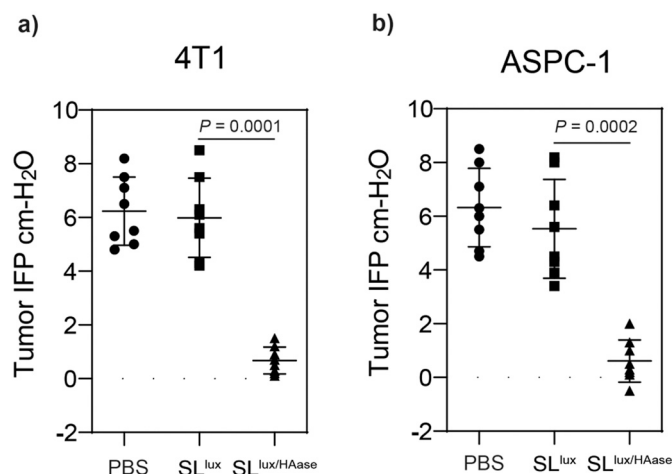


Fig. 3. HAase-expressing bacteria decrease tumor IFP in 4T1 and ASPC-1 tumor tissues. BALB/c or BALB/c athymic nu-/nu- mice ($n = 8$ per group) received subcutaneous injections of 4T1 (1×10^6) or ASPC-1 (1×10^7) cells. When the tumor volumes reached approximately 150 mm^3 , the tumor-bearing mice were injected with PBS, SL^{lux} , or $\text{SL}^{\text{lux/HAase}}$ followed by intraperitoneal injections of L -arabinose at 4 days post infection (DPI). After excising the tumor tissues at 6 DPI (tumor volume = $100\text{--}200 \text{ mm}^3$), IFP was measured. a) IFP of 4T1 tumor tissues in PBS, SL^{lux} , or $\text{SL}^{\text{lux/HAase}}$. b) IFP of ASPC-1 tumor tissues in PBS, SL^{lux} , or $\text{SL}^{\text{lux/HAase}}$. IFP measurements are given in $\text{cm-H}_2\text{O}$. Boxes represent the quartiles, and whiskers mark the 10th to 90th percentiles. IFP, Interstitial fluid pressure; SL^{lux} , *Salmonella* carrying an empty vector; $\text{SL}^{\text{lux/HAase}}$, HAase-expressing *Salmonella* with L -arabinose induction.

chemotherapeutic drugs, presence of *Salmonella* was detected in both tumor models (Fig. S4 and S5). In both the 4T1 and ASPC-1 tumor models, the treatments resulted in tumor growth suppression and tumor shrinkage (Figs. 4b and 5b, Figs. S4a and S5a). Strong bioluminescence signals originating from the chromosomal *lux* operon of *Salmonella* were detected specifically in the tumors of mice injected with bacteria (Figs. 4c and 5c, Figs. S4b and S5b). Among mice treated with $\text{SL}^{\text{lux/HAase}}$, in the groups combined with chemotherapeutic drugs (gemcitabine, doxorubicin, and/or paclitaxel), in the presence of L -arabinose, tumor growth in the 4T1 mouse model was significantly reduced compared with that in other groups. In contrast, no significant reduction in tumor growth in the $\text{SL}^{\text{lux/HAase}}$ group combined with paclitaxel was observed (Fig. S4c and d). At the end of the treatment regimen, in both models, the tumor volume was determined in the following three groups: (i) PBS, (ii) only chemotherapeutic drugs (gemcitabine, doxorubicin, and/or paclitaxel), engineered bacteria (SL^{lux} , $\text{SL}^{\text{lux/HAase}}$), engineered bacteria without L -arabinose ($\text{SL}^{\text{lux/HAase(-)}}$) combined with doxorubicin and combined $\text{SL}^{\text{lux/HAase}}$ with paclitaxel, and (iii) combined $\text{SL}^{\text{lux/HAase}}$ with gemcitabine or doxorubicin. Statistical P values for all groups are as follows: group (i, PBS) vs. group (iii, $\text{SL}^{\text{lux/HAase}}$ with doxorubicin), $P = 0.0002$ (in 4T1), $P = 0.0005$ (in ASPC-1); group (i, PBS) vs. group (ii, SL^{lux}), $P = 0.0127$ (in 4T1), group (i, PBS) vs. group (ii, doxorubicin) $P = 0.0015$ (in ASPC-1); group (ii, doxorubicin or $\text{SL}^{\text{lux/HAase(-)}} + \text{Doxo}$) vs. group (iii, $\text{SL}^{\text{lux/HAase}}$ with doxorubicin), $P = 0.0014$ (in 4T1), group (ii, $\text{SL}^{\text{lux/HAase}}$ or $\text{SL}^{\text{lux/HAase(-)}} + \text{Doxo}$) vs. group (iii, $\text{SL}^{\text{lux/HAase}}$ with doxorubicin), $P = 0.0024$ (in ASPC-1). In the 4T1 tumor model, the mean tumor volumes after 25 days of treatment were 126 or 132 mm^3 , respectively, for the group treated with combined $\text{SL}^{\text{lux/HAase}}$ with gemcitabine or doxorubicin in the presence of L -arabinose (Fig. 4d and Fig. S4c). Moreover, the mean tumor volume in the group treated with combined $\text{SL}^{\text{lux/HAase}}$ in the presence of L -arabinose with paclitaxel was 530 mm^3 , which suggested that the combination of $\text{SL}^{\text{lux/HAase}}$ with paclitaxel had no synergistic effect (Fig. S4c and d). In the ASPC-1 tumor model, the mean tumor volumes after 25 days of treatment were 196 or 212 mm^3 , respectively, for the group treated with combined $\text{SL}^{\text{lux/HAase}}$ in the presence of L -arabinose with doxorubicin or gemcitabine (Fig. 5d

and Fig. S5c). Additionally, in both 4T1 and ASPC-1 models, the survival rates were considerably higher in mice groups that received a combination of $\text{SL}^{\text{lux/HAase}}$ with gemcitabine or doxorubicin compared to those in other groups (Figs. 4e and 5e, Figs. S4d and S5d). Tumor shrinkage and survival time were significantly lower in the group treated with only chemotherapeutic drug groups (gemcitabine, doxorubicin, and/or paclitaxel) than those in the groups of $\text{SL}^{\text{lux/HAase}}$ combined with an ECM-targeting bacteria with chemotherapeutics. This indicates that combination therapy with ECM-targeting bacteria and chemotherapeutic drugs (doxorubicin and gemcitabine) have the potential to enhance their antitumor therapeutic effects. Immunofluorescence staining revealed that most of the tumor HA was degraded and hardly detected in tumor-bearing mice groups treated with HAase-expressing bacteria ($\text{SL}^{\text{lux/HAase}}$) compared to those treated with PBS and SL^{lux} (Figs. S6 and S7). To confirm HAase activity in ECM of tumor, we also performed *ex vivo* HAase activity assays of tumor tissues in ASPC-1 tumor-bearing mice (Fig. S8), which indicated that HAase activity was increased after bacterial injection. These results suggest that HAase-expressing bacteria target tumors, degrade HA in the ECM of tumors, decrease the IFP of tumors, and exert elevated tumor suppression effects when combined with chemotherapeutic drugs. High IFP has been reported to be a substantial barrier to drug delivery in solid tumors. We speculate that the combination therapy of ECM-targeted bacteria and chemotherapeutic drugs (doxorubicin and gemcitabine) decreased tumor IFP and improved tumor treatment efficacy. Therefore, these findings reveal a potential functional mechanism for the enhanced antitumor effects of engineered bacteria combined with chemotherapeutic drugs.

3.5. HAase inhibits HA binding to its receptor CD44, which regulates proliferation and apoptosis of tumor cells

HA increased in the tumor microenvironment promotes tumor cell proliferation, invasion, immune evasion, stemness alterations, and drug resistance [52]. We explored whether decreased level of HA modulates the level of its receptor, the transmembrane protein CD44. We also evaluated cell proliferation and apoptosis. Immunofluorescence analysis of the ASPC-1 tumors revealed that the HAase expressed in engineered bacteria degraded HA in tumor ECM and decreased the level of CD44 (Fig. 6a). Similar findings were made in western blot analyses (Fig. 6b). Interestingly, the level of Ki-67, a cell proliferation biomarker, was also significantly reduced in tumor tissues injected with $\text{SL}^{\text{lux/HAase}}$ with doxorubicin (Fig. 6). Furthermore, TUNEL staining showed that apoptosis was induced in HAase-expressed engineered bacteria. Collectively, these results demonstrated that tumor HA was degraded by HAase secreted from injected $\text{SL}^{\text{lux/HAase}}$, which may reduce the interaction between HA and CD44. We speculate that tumor HA degradation by $\text{SL}^{\text{lux/HAase}}$ may lead to inhibition of the proliferation-inducing signaling pathway, which is the downstream of CD44 signaling pathway, induce apoptosis, and decrease the CD44 level of tumors.

3.6. Systemic toxicity of HAase-expressing *Salmonella*

S. typhimurium is a tumor-targeting therapeutic agent and a carrier for drugs [5]. A previous study reported that an engineered bacterium carrying ClyA potentially caused hepatic injury immediately after injection [6]. ClyA, a 34 kDa pore-forming hemolytic protein produced by *E. coli*, *S. typhimurium*, and *S. paratyphi* A, can be transported to the bacterial surface and secreted without post-translational modification. In the present study, we designed the carrier using ECM-degrading drugs rather than cytotoxic drugs. To confirm whether ECM-targeting bacteria had a cytotoxic effect in ASPC-1 tumor-bearing mice, we examined the hepatic or splenic injuries following injection of HAase-expressing *Salmonella*. To do this, we monitored the clinical chemistry plasma markers: CRP and procalcitonin. Furthermore, we performed immunofluorescence staining of the liver. The engineered bacteria were

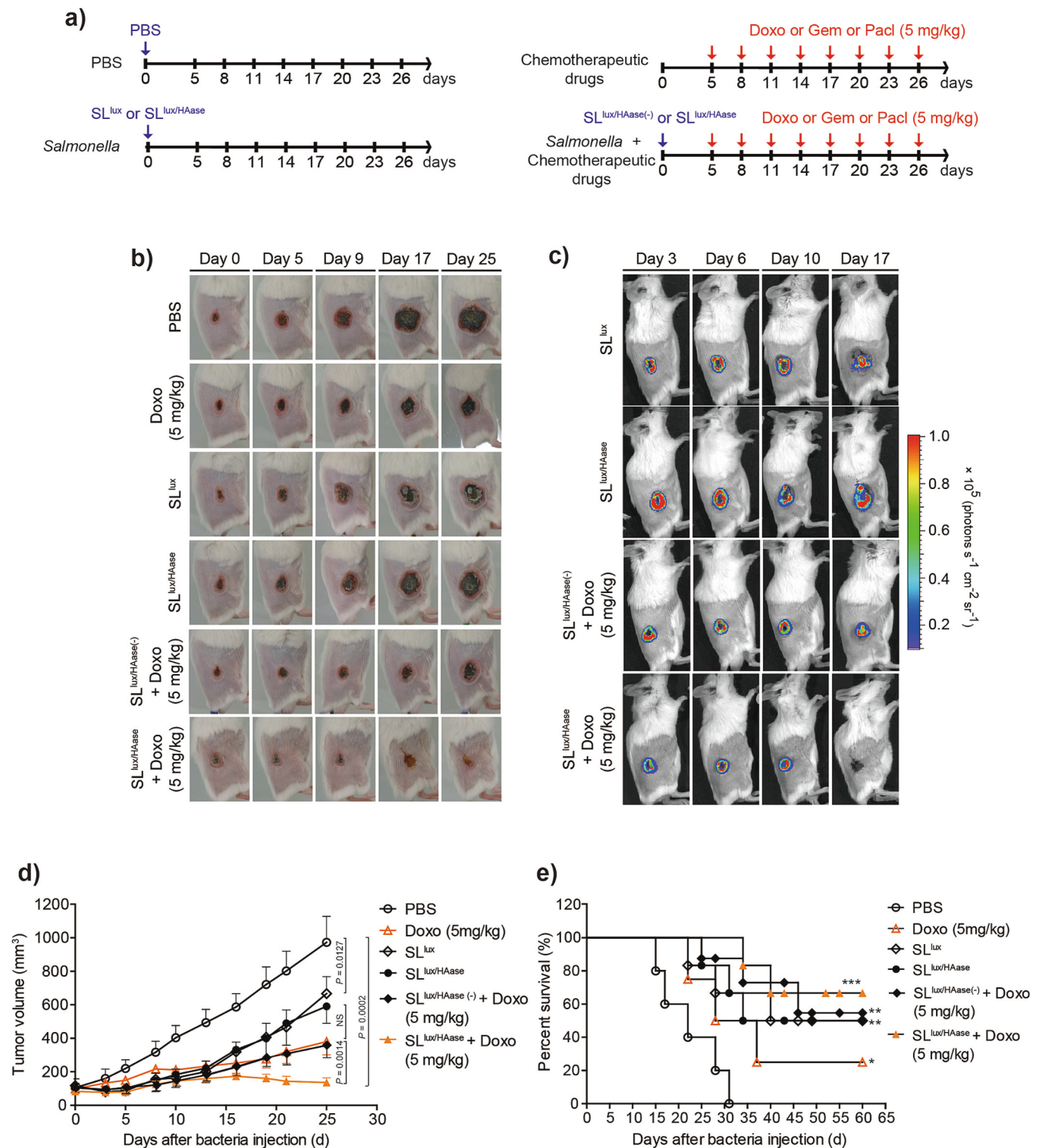


Fig. 4. *In vivo* imaging and tumor-suppressive effects of HAase-expressing bacteria combined with doxorubicin in 4T1 tumor-bearing mice. BALB/c mice ($n = 15$ per group) received subcutaneous injections of 4T1 (1×10^6) cells. When the tumor volumes reached approximately 120 mm^3 , the mice were divided into six treatment groups: PBS alone, chemotherapeutic drug (Doxo) alone, bacteria group (SL^{lux} or $\text{SL}^{\text{lux/HAase}}$), and HAase-expressing bacteria with (+) or without (–) L-arabinose induction, and with chemotherapeutic drug ($\text{SL}^{\text{lux/HAase(-)}} + \text{Doxo}$ and $\text{SL}^{\text{lux/HAase}} + \text{Doxo}$). Mice were then treated with engineered bacteria (1×10^7) and a chemotherapeutic drug (5 mg/kg) by intravenous injections. The tumor-bearing mice administrating bacteria received a daily intraperitoneal injection of 60 mg L-arabinose (0.2% final concentration), starting at 4 days post infection (DPI). a) Injection schedule of the chemotherapeutic drugs. b) Representative photographs of subcutaneous tumors in mice from different treatment groups. c) Representative non-invasive *in vivo* imaging of bacterial bioluminescence. d) Graphs depicting changes in the tumor volume over time after injections with bacteria. (E) Kaplan–Meier survival curves for 4T1 tumor-bearing mice. Statistical significance was calculated by comparing other treatment groups with the PBS group. * $P < 0.01$, ** $P < 0.001$, *** $P < 0.0001$. Doxo, Doxorubicin; SL^{lux} , *Salmonella* carrying an empty vector; $\text{SL}^{\text{lux/HAase}}$, HAase-expressing *Salmonella* with L-arabinose induction; $\text{SL}^{\text{lux/HAase(-)}} + \text{Doxo}$, HAase-expressing *Salmonella* without L-arabinose induction plus Doxorubicin (5 mg/kg); $\text{SL}^{\text{lux/HAase}} + \text{Doxo}$, HAase-expressing *Salmonella* with L-arabinose induction plus Doxorubicin (5 mg/kg).

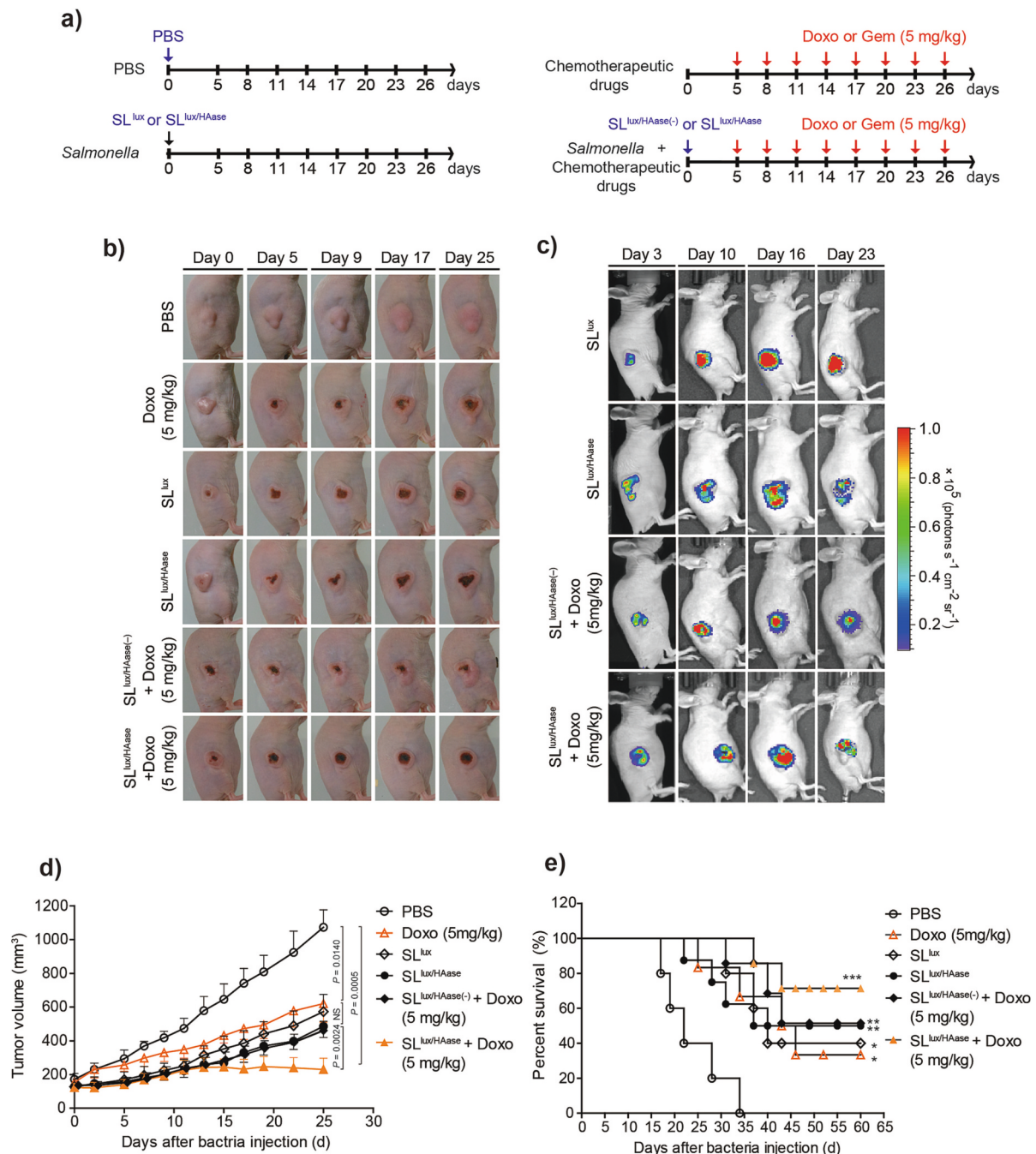


Fig. 5. *In vivo* imaging and tumor-suppressive effects of HAase-expressing bacteria combined with doxorubicin in ASPC-1 tumor-bearing mice. BALB/c athymic nu/nu- mice ($n = 20$ per group) received subcutaneous injections of ASPC-1 (1×10^7) cells. When the tumor volumes reached approximately 130 mm^3 , mice were divided into six treatment groups: PBS alone, chemotherapeutic drug (Doxo) alone, bacteria group (SL_{lux} or SL_{lux/HAase}), and HAase-expressing bacteria with (+) or without (−) L-arabinose induction, and with chemotherapeutic drug (SL_{lux/HAase(-)} plus Doxo and SL_{lux/HAase} plus Doxo). The mice were then treated with engineered bacteria (3×10^7 CFU) and chemotherapeutic drug (5 mg/kg) by intravenous injections. The group with the bacteria-colonized tumor-bearing mice received a daily intraperitoneal injection of 60 mg L-arabinose (0.2% final concentration), starting at 4 DPI. a) Injection schedule of the chemotherapeutic drugs. b) Representative photographs of subcutaneous tumors in mice from different treatment groups. c) Representative images showing non-invasive *in vivo* imaging of bacterial bioluminescence. d) Graphs showing changes in the tumor volume over time after injections with bacteria. e) Kaplan–Meier survival curves for 4T1 tumor-bearing mice. Statistical significance was calculated by comparison with PBS or other groups. $*P < 0.01$, $**P < 0.001$, $***P < 0.0001$. Doxo, Doxorubicin; SL_{lux}, *Salmonella* carrying an empty vector; SL_{lux/HAase}, HAase-expressing *Salmonella* with L-arabinose induction; SL_{lux/HAase(-)} + Doxo, HAase-expressing *Salmonella* without L-arabinose induction plus Doxorubicin (5 mg/kg); SL_{lux/HAase} + Doxo, HAase-expressing *Salmonella* with L-arabinose induction plus Doxorubicin (5 mg/kg).

intravenously injected into BALB/c nu/nu- mice bearing ASPC-1 tumors. HAase expression was induced by tail vein administration of L-arabinose on the day of bacterial injection (0 DPI) or at 3 DPI. At 5 DPI, serum levels of aspartate aminotransferase (AST) and alanine aminotransferase (ALT) in the mice that received L-arabinose at 0 DPI were

significantly elevated compared with those in mice that received it at 3 DPI ($P < 0.01$) (Fig. S9). The markers of inflammation or infection, such as CRP and procalcitonin, were within the normal ranges in all experimental groups (Fig. S9). These results provided evidence that the controlled induction of HAase by L-arabinose at 3 DPI did not cause

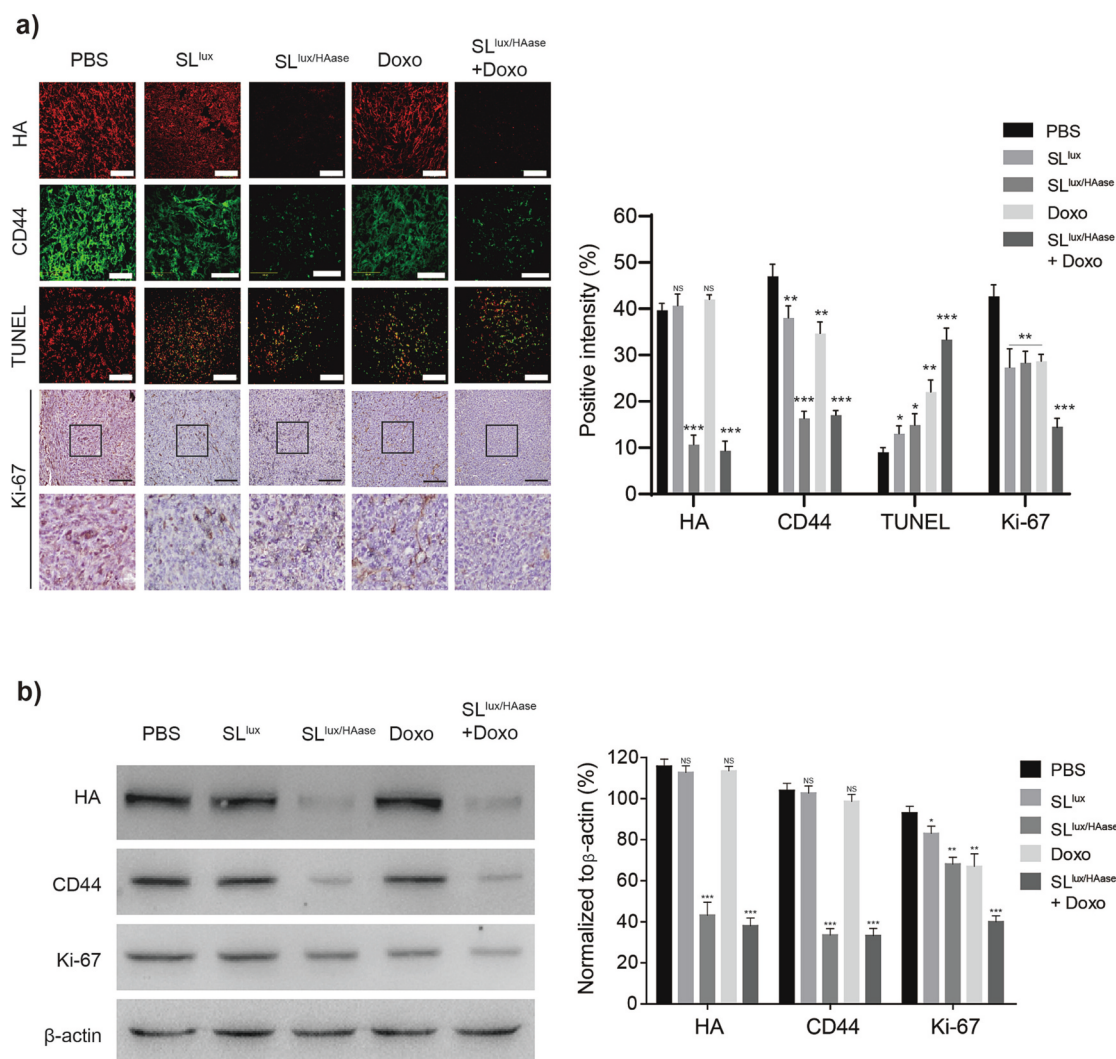


Fig. 6. HAase-expressing bacteria inhibit binding of hyaluronan to CD44, regulating proliferation and apoptosis of tumor cells. BALB/c athymic nu-/nu- mice ($n = 8$ per group) received subcutaneous injections of ASPC-1 (1×10^7) cells. When the tumor volumes reached approximately 130 mm^3 , the tumor-bearing mice were injected with PBS alone, SL^{lux}, SL^{lux}/HAase, chemotherapeutic drug (Doxo) alone, or SL^{lux}/HAase plus Doxo, followed by intraperitoneal injections of L-arabinose at 4 days post infection (DPI). Immunofluorescence and immunohistochemical study ($n = 4$ per group) or immunoblot analysis ($n = 4$ per group) were performed after excising the tumor grafts treated with *S. typhimurium*. **a)** Immunofluorescence staining with HABP (red), anti-CD44 antibody (green), and DAPI/antifade (blue) as well as immunohistochemical staining with the HRP-conjugated anti-Ki-67 antibody in ASPC-1 tumors from mice injected with PBS, SL^{lux}, or SL^{lux}/HAase plus doxorubicin at 12 DPI. TUNEL staining was performed with FITC-dUTP (green) and propidium iodide was used as a counterstain. Representative merged image is shown (overlay). Scale bar for HA, CD44, and TUNEL = $100 \mu\text{m}$. Scale bar for Ki-67 = $200 \mu\text{m}$. **b)** Immunoblot analysis of HA, CD44, and Ki-67 antibodies in the tumors (see Table S2). Data are representative of three independent experiments. Doxo, Doxorubicin; SL^{lux}, *Salmonella* carrying an empty vector; SL^{lux}/HAase, HAase-expressing *Salmonella* with L-arabinose induction; SL^{lux}/HAase + Doxo, HAase-expressing *Salmonella* with L-arabinose induction plus Doxorubicin (5 mg/kg). * $P < 0.01$, ** $P < 0.001$, *** $P < 0.0001$ (versus PBS group). (For interpretation of the references to colour in this figure legend, the reader is referred to the web version of this article.)

hepatic injury. The immunofluorescence analysis also showed no significant degradation of HA in the livers harboring tumor-targeting bacteria (Fig. S10).

Overall, we considered that ECM-targeting bacteria expressing HAase did not cause serious toxicity in the liver and had high biosafety when applied in cancer immunotherapy. Unfortunately, serum levels could not be measured when bacteria and chemotherapeutic drugs were combined. However, histological staining of liver tissue showed that liver HA was not degraded even though bacteria in the SL^{lux}/HAase + Dox group were present in low concentrations in liver (Fig. S10). The results indicate that ECM-targeting bacterial therapy did not induce severe inflammatory reactions."

4. Discussion

HAase-expressing *Salmonella* targets and degrades the tumor microenvironment. They also exert enhanced tumor suppression effects in combination with anticancer agents. To date, BCT strategies have mainly been developed to express anticancer drugs, such as those involving bacterial cytotoxic agents, cytokines, antigens, and immunomodulators [9,18,53]. Chemotherapy alone has also been explored to enhance tumor suppression; however, synergistic effects with BCT strategies have not been demonstrated. In this study, we hypothesized that HAase-expressing *Salmonella* would effectively diffuse chemotherapeutic drugs within tumors by lowering the IFP. HAase secretion from *Salmonella* (known as active therapy) is a promising candidate for treatment in combination with chemotherapy. This is because it degrades the ECM by lysing HA within tumor tissues, which facilitates

enhanced drug delivery. We demonstrated that HAase secretion from such bacteria resulted in a decrease in the IFP in tumor tissues via HA degradation (Fig. 3). Additionally, a combination of chemotherapeutic drugs, such as doxorubicin and gemcitabine (known as passive therapy), showed tumor-suppressive effects superior to their individual effects. We also confirmed that chemotherapeutic drugs, when delivered systemically, are capable of preferentially diffusing into breast and pancreatic cancers in mice. This results in synergistic tumor suppression, when combined with BCT.

HA also plays a major role as a signaling molecule in tumor progression that activates intracellular pathways and promotes cell motility and proliferation [52]. Jacobetz et al. [34] demonstrated that HA depletion by the PEGylated form of human HAase (PEGPH20) induces re-expansion of blood vessels, increases the delivery of anticancer agents, and promotes tumor-specific increase in macromolecule permeability. However, the high risk of adverse effects associated with systemically delivered HAase, such as ECM degradation in healthy tissues, remains a major concern. To reduce these risks, lower doses of HAase must be administered; however, this may not necessarily maximize the therapeutic efficacy. In the present study, we designed a carrier that could degrade HA in tumor ECM by expressing HAase, using tumor-targeting bacterium *S. typhimurium*. Furthermore, by tightly regulating and expressing HAase, it was able to overcome the disadvantages of direct PEGPH20 injection and treat cancer effectively and safely. When bacteria are initially administered via the tail vein and are transiently localized in RES organs, bacterial toxicity is the most important safety issue. Moreover, stringent regulatory approval would be required for the application of this approach in clinical settings. Therefore, bacteria-derived cytotoxic drugs should only be introduced when bacteria have been cleared from reticuloendothelial cells and accumulated in the targeted tumor tissues. In this study, to avoid systemic toxicity, bacterial expression systems were regulated using inducible promoters. HAase-targeting bacteria, tightly regulated by the induction system, could colonize and proliferate within the tumor after 3 DPI. Early induction of HAase (0 DPI) induced hepatic toxicity. However, when HAase expression was induced at 3 DPI, the tested clinical parameters were within their normal ranges (Fig. S9). Based on Figs. S9 and S10, the ALT and AST levels are increased when HAase expression is induced by L-arabinose at the time of bacterial injection (0 DPI) potentially because the induced HAase degrades HA of liver. However, since the bacterial clearance mechanisms occur from the liver consisting of RES, low levels of bacteria are expected in the liver 3 days after bacterial injection. This is why hepatic injury may not have occurred despite HAase induction on 3 DPI.

Furthermore, we examined the biodistribution after injection of ECM-targeting *Salmonella* in 4T1 tumor-bearing mice (Fig. S11). Fig. S11 shows that administered bacteria were cleared from the RES organs, such as the liver and spleen, and began to proliferate in tumors 3–4 days after injection. Therefore, HAase should be induced only when the bacteria have cleared from RES organs and accumulated in targeted tumor tissue; this normally occurred 3–4 days after administration. This could be the reason why hepatic injury did not occur despite HAase induction on 3 DPI. Taken together, results for systemic cytotoxicity (Figs. S9 and S10) and biodistribution (Fig. S11) were suggestive of the absence of serious inflammation or sepsis, furthermore, our murine *in vivo* experiments further indicated that engineered bacteria regulated by inducible promoters are safe for use in therapeutics and are promising chemotherapeutic drugs. Flow cytometry analysis also showed a drastic increase in neutrophil, macrophage, CD4⁺, and CD8⁺ T lymphocyte infiltration in 4T1 tumor tissues (Fig. S12). In addition, SL^{lux/HAase} significantly promoted the secretion of inflammatory cytokines, such as interleukin IL-1 β and tumor necrosis factor TNF- α (Fig. S13). Furthermore, changes in the immune cell population and the levels of inflammatory cytokines were observed more clearly in combination therapy with SL^{lux/HAase} and the chemotherapeutic drug doxorubicin (SL^{lux/HAase} + Doxo). These results indicate that bacterial therapy using SL^{lux/HAase}

exhibited the potential to recruit large amounts of immune cells and alleviate the immunosuppressive state. Unfortunately, as the ASPC-1 tumor model was of BALB/c athymic nu-/nu- mice, the changes in the immune cell population and the levels of inflammatory cytokines could not be determined in ASPC-1 tumor tissues.

Our *in vivo* results indicated that HAase-expressing bacteria colonized in cancer cells and suppressed their growth via ECM degradation. Combination of SL^{lux/HAase} with chemotherapeutic drugs, such as doxorubicin or gemcitabine, had a synergistic effect by enhancing tumor suppression and prolonging survival. However, SL^{lux/HAase} combined with paclitaxel had no synergistic tumor-suppressive effects in the breast cancer models (4T1-derived). In clinical trials with a PEGylated recombinant human HAase (PEGPH20), a significant increase in tumor-suppressive effects was reported when combined with gemcitabine and abraxane, a nanoparticle albumin-bound paclitaxel (nab-paclitaxel) [54]. Paclitaxel is a highly hydrophobic agent, and the available formulations require organic compounds for its dissolution. In contrast, nab-paclitaxel is a solvent-free formulation used for treating breast cancer that quickly dissolves into smaller endogenous albumin-sized (approximately 10 nm) complexes. This results in greater activity and better safety profiles [55]. Therefore, findings regarding the paclitaxel treatment in this study may explain why the efficacy of bacterial tumor therapy was limited to certain groups of chemotherapeutic drugs (doxorubicin and gemcitabine) in the 4T1 tumor-bearing mice.

HA accumulates in the stroma of various tumors and modulates intracellular signaling pathways, proliferation, motility, and invasive properties of the malignant cells [31,52]. Cell proliferation is associated with the binding of HA to its receptor CD44, which stimulates the PI3K/Akt pathway activity [56]. Here, we demonstrated that HAase expression inhibited the binding of HA and CD44 in the ASPC-1 mouse model. Furthermore, it inhibited the proliferation and induced apoptosis of tumor cells. Notably, when treated with HAase-targeting bacteria combined with a combined chemotherapeutic effect, the decrease in CD44 levels observed in our *ex vivo* experiments indicates that it may inhibit tumor cell proliferation as well as tumor cell adhesion and invasion.

Several therapies are being developed to treat cancer, including those based on nanoparticles, antibodies, chemotherapeutic combinations, viruses, and bacteria. When combined with chemotherapeutic drugs, BCT and HAase-expressing *Salmonella* have shown excellent anticancer effects in mice harboring HA-rich tumors. This suggests that these strategies could be applied to a broad spectrum of malignancies to suppress tumor progression. We developed a strategy of ECM-degrading cytotoxic drug expression that modulates the tumor microenvironment, thus providing a platform to increase the number of potential therapeutic combinations to maximize efficacy. Moreover, we demonstrated that HAase-expressing *Salmonella* can target tumor-specific HA in pancreatic and breast tumors and increase the penetration of chemotherapeutic drugs via lowering the IFP. This approach is based on the cooperative activity of SL and HAase, in combination with chemotherapeutic drugs. Bacterial colonization in tumors induces tumor infiltration of chemotherapeutic drugs and subsequently suppresses tumor growth and prolongs survival. Thus, localized production of HAase combined with chemotherapeutic drug delivery exerts a powerful and synergistic anticancer effect. Combination therapy, which exerts synergistic effects of bacterial “active” therapy and anticancer drug “passive” therapy may, therefore, enhance the tumor therapeutic effects via ECM modulation.

5. Conclusions

We engineered a bacterium that expresses and secretes HAase. This engineered ECM-targeting *Salmonella* effectively degraded HA, a major ECM constituent in tumors. Combining engineered bacteria with chemotherapeutic drugs (doxorubicin or gemcitabine) suppressed tumor growth and prolonged survival in mouse models of both

pancreatic adenocarcinoma ASPC-1 and breast cancer 4T1. The HAase-mediated ECM degradation decreased the IFP in the tumor microenvironment, indicating that the limitations of chemotherapy can be overcome through this strategy. Additionally, immunofluorescence and immunoblot analyses revealed that levels of the proliferation marker Ki-67 decreased, and apoptosis was promoted in SL^{lux}/HAase-injected mice. We expect that HA degradation using HAase-expressing *Salmonella in vivo* decreased interactions between HA and CD44 receptor. This might have resulted in inhibition of the CD44-mediated signaling pathway, which regulates cell proliferation and apoptosis. Therefore, this ECM-targeting bacteria can be used as a synergistic anticancer therapeutic agent to maximize chemotherapeutic drug delivery into highly invasive tumors. This was achieved by inhibiting the IFP and to enhance the antitumor efficacy of chemotherapeutic drugs. This ECM-targeting and -degrading technology based on oncolytic bacteria is a prospective approach to drug penetration management in the future, which will significantly improve the outcomes of various oncology therapies.

Funding

The research was supported by the Bio & Medical Technology Development Program of the National Research Foundation (NRF) funded by the Ministry of Science, ICT & Future Planning (NRF-2014M3A9B5073747, NRF-2021M3H9A1037439) and a grant from the Korea Research Institute of Bioscience & Biotechnology (KRIBB) Research initiative program (KGM5232221, NTIS1711170602). S.-H.P. was supported by the Technology Innovation Program (20009412, Discovery and fermentation optimization of uncultured bacteria from gut microbiome based on genomic big data) funded by the Ministry of Trade, Industry and Energy (MOTIE, Republic of Korea).

CRediT authorship contribution statement

Ji-Sun Kim: Methodology, Investigation, Writing – original draft. **Jam-Eon Park:** Methodology, Data curation. **Seung-Hyeon Choi:** Methodology, Data curation. **Se Won Kang:** Formal analysis. **Ju Huck Lee:** Visualization. **Jung-Sook Lee:** Resources. **Minsang Shin:** Methodology. **Seung-Hwan Park:** Conceptualization, Methodology, Investigation, Data curation, Writing – original draft, Supervision, Funding acquisition.

Declaration of Competing Interest

The authors declare that no competing interest exists.

Data availability

Data will be made available on request.

Acknowledgments

We thank the staff of KBSI (Gwangju, Korea) for technical assistance in IVIS spectrum analysis.

Appendix A. Supplementary data

Supplementary data to this article can be found online at <https://doi.org/10.1016/j.jconrel.2023.02.001>.

References

- [1] N.J. Roberts, L. Zhang, F. Janku, A. Collins, R.-Y. Bai, V. Staedtke, A.W. Rusk, D. Tung, M. Miller, J. Roix, K.V. Khanna, R. Murthy, R.S. Benjamin, T. Helgason, A. D. Szvalb, J.E. Bird, S. Roy-Chowdhuri, H.H. Zhang, Y. Qiao, B. Karim, J. McDaniel, A. Elpiner, A. Sahara, J. Lachowicz, B. Phillips, A. Turner, M.K. Klein, G. Post, L.A. D. Jr, G.J. Riggins, N. Papadopoulos, K.W. Kinzler, B. Vogelstein, C. Bettingowda, D. L. Huso, M. Varterasian, S. Saha, S. Zhou, Intratumoral injection of *Clostridium* novyi-NT spores induces antitumor responses, *Sci. Transl. Med.* 6 (2014) 249ra111, <https://doi.org/10.1126/scitranslmed.3008982>.
- [2] L. Wang, Q. Wang, X. Tian, X. Shi, Learning from *Clostridium novyi* -NT: how to defeat cancer, *J. Canc. Res. Ther.* 14 (2018) 1, <https://doi.org/10.4103/0973-1482.204841>.
- [3] B.C. Selvanesan, D. Chandra, W. Quispe-Tintaya, A. Jahangir, A. Patel, K. Meena, R.A.A.D. Silva, M. Friedman, L. Gabor, O. Khouri, S.K. Libutti, Z. Yuan, J. Li, S. Siddiqui, A. Beck, L. Tesfa, W. Koba, J. Chuy, J.C. McAuliffe, R. Jafari, D. Entenberg, Y. Wang, J. Condeelis, V. DesMarais, V. Balachandran, X. Zhang, K. Lin, C. Gravekamp, *Listeria* delivers tetanus toxoid protein to pancreatic tumors and induces cancer cell death in mice, *Sci. Transl. Med.* 14 (2022) eabc1600, <https://doi.org/10.1126/scitranslmed.abc1600>.
- [4] M. Zhao, M. Yang, X.-M. Li, P. Jiang, E. Baranov, S. Li, M. Xu, S. Penman, R. M. Hoffman, Tumor-targeting bacterial therapy with amino acid auxotrophs of GFP-expressing *Salmonella typhimurium*, *Proc. Natl. Acad. Sci. U. S. A.* 102 (2005) 755–760, <https://doi.org/10.1073/pnas.0408422102>.
- [5] J.H. Zheng, V.H. Nguyen, S.-N. Jiang, S.-H. Park, W. Tan, S.H. Hong, M.G. Shin, I.-J. Chung, Y. Hong, H.-S. Bom, H.E. Choy, S.E. Lee, J.H. Rhee, J.-J. Min, Two-step enhanced cancer immunotherapy with engineered *Salmonella typhimurium* secreting heterologous flagellin, *Sci. Transl. Med.* 9 (2017) eaak9537, <https://doi.org/10.1126/scitranslmed.aak9537>.
- [6] S.N. Jiang, S.H. Park, H.J. Lee, H.J. Zheng, H.S. Kim, H.S. Bom, Y. Hong, M. Szardenings, M.G. Shin, S.C. Kim, V. Ntziachristos, H.E. Choy, J.J. Min, Engineering of bacteria for the visualization of targeted delivery of a cytolytic anticancer agent, *Mol. Ther.* 21 (2013) 1985–1995, <https://doi.org/10.1038/mt.2013.183>.
- [7] S.-N. Jiang, T.X. Phan, T.-K. Nam, V.H. Nguyen, H.-S. Kim, H.-S. Bom, H.E. Choy, Y. Hong, J.-J. Min, Inhibition of tumor growth and metastasis by a combination of *Escherichia coli*-mediated cytolytic therapy and radiotherapy, *Mol. Ther.* 18 (2010) 635–642, <https://doi.org/10.1038/mt.2009.295>.
- [8] H. Zhu, Z. Li, S. Mao, B. Ma, S. Zhou, L. Deng, T. Liu, D. Cui, Y. Zhao, J. He, C. Yi, Y. Huang, Antitumor effect of sFlt-1 gene therapy system mediated by *Bifidobacterium infantis* on Lewis lung cancer in mice, *Cancer Gene Ther.* 18 (2011) 884–896, <https://doi.org/10.1038/cgt.2011.57>.
- [9] W. Tan, M.T.-Q. Duong, C. Zuo, Y. Qin, Y. Zhang, Y. Guo, Y. Hong, J.H. Zheng, J.-J. Min, Targeting of pancreatic cancer cells and stromal cells using engineered oncolytic *Salmonella typhimurium*, *Mol. Ther.* 30 (2022) 662–671, <https://doi.org/10.1016/j.jymthe.2021.08.023>.
- [10] P. Chorobik, D. Czaplicki, K. Ossysek, J. Bereta, *Salmonella* and cancer: from pathogens to therapeutics, *Acta Biochim. Pol.* 60 (2013), <https://doi.org/10.18388/abp.2013.1984>.
- [11] J.F. Toso, V.J. Gill, P. Hwu, F.M. Marincola, N.P. Restifo, D.J. Schwartzentruber, R. M. Sherry, S.L. Topalian, J.C. Yang, F. Stock, L.J. Freezer, K.E. Morton, C. Seipp, L. Haworth, S. Mavroukakis, D. White, S. MacDonald, J. Mao, M. Sznol, S. A. Rosenberg, Phase I study of the intravenous administration of attenuated *Salmonella typhimurium* to patients with metastatic melanoma, *J. Clin. Oncol.* 20 (2002) 142–152.
- [12] T. Murakami, Y. Hiroshima, Y. Zhang, M. Zhao, T. Kiyuna, H.K. Hwang, K. Miyake, Y. Homma, R. Mori, R. Matsuyama, T. Chishima, Y. Ichikawa, K. Tanaka, M. Bouvet, I. Endo, R.M. Hoffman, Tumor-targeting *Salmonella typhimurium* A1-R promotes tumoricidal CD8⁺ T cell tumor infiltration and arrests growth and metastasis in a syngeneic pancreatic-cancer orthotopic mouse model, *J. Cell. Biochem.* 119 (2018) 634–639, <https://doi.org/10.1002/jcb.26224>.
- [13] Y. Hiroshima, M. Zhao, Y. Zhang, A. Maawy, M. Hassanein, F. Uehara, S. Miwa, S. Yano, M. Momiyama, A. Suetsugu, T. Chishima, K. Tanaka, M. Bouvet, I. Endo, R.M. Hoffman, Comparison of efficacy of *Salmonella typhimurium* A1-R and chemotherapy on stem-like and non-stem human pancreatic cancer cells, *Cell Cycle* 12 (2013) 2774–2780, <https://doi.org/10.4161/cc.25872>.
- [14] M. Song, H.-J. Kim, E.Y. Kim, M. Shin, H.C. Lee, Y. Hong, J.H. Rhee, H. Yoon, S. Ryu, S. Lim, H.E. Choy, ppGpp-dependent stationary phase induction of genes on *Salmonella* pathogenicity island 1, *J. Biol. Chem.* 279 (2004) 34183–34190, <https://doi.org/10.1074/jbc.m313491200>.
- [15] M. Zhao, M. Yang, H. Ma, X. Li, X. Tan, S. Li, Z. Yang, R.M. Hoffman, Targeted therapy with a *Salmonella typhimurium* leucine-arginine auxotroph cures orthotopic human breast tumors in nude mice, *Cancer Res.* 66 (2006) 7647–7652, <https://doi.org/10.1158/0008-5472.can-06-0716>.
- [16] N.S. Forbes, Engineering the perfect (bacterial) cancer therapy, *Nat. Rev. Cancer* 10 (2010) 785–794, <https://doi.org/10.1038/nrc2934>.
- [17] V.H. Nguyen, H.-S. Kim, J.M. Ha, Y. Hong, H.E. Choy, J.J. Min, Genetically engineered *Salmonella typhimurium* as an imageable therapeutic probe for cancer, *Cancer Res.* 70 (2010) 18–23, <https://doi.org/10.1158/0008-5472.can-09-3453>.
- [18] J.-E. Kim, T.X. Phan, V.H. Nguyen, H.-V. Dinh-Vu, J.H. Zheng, M. Yun, S.-G. Park, Y. Hong, H.E. Choy, M. Szardenings, W. Hwang, J.-A. Park, S. Park, S.-H. Im, J.-J. Min, *Salmonella typhimurium* suppresses tumor growth via the pro-inflammatory cytokine interleukin-1 β , *Theranostics* 5 (2015) 1328–1342, <https://doi.org/10.7150/thno.11432>.
- [19] J.-J. Min, V.H. Nguyen, H.-J. Kim, Y. Hong, H.E. Choy, Quantitative bioluminescence imaging of tumor-targeting bacteria in living animals, *Nat. Protocols* 3 (2008) 629–636, <https://doi.org/10.1038/nprot.2008.32>.
- [20] C.-H. Lee, C.-L. Wu, A.-L. Shiao, Endostatin gene therapy delivered by *Salmonella choleraesuis* in murine tumor models, *J. Gene Med.* 6 (2004) 1382–1393, <https://doi.org/10.1002/jgm.626>.
- [21] S.H. Park, J.H. Zheng, V.H. Nguyen, S.N. Jiang, D.Y. Kim, M. Szardenings, J. H. Min, Y. Hong, H.E. Choy, J.J. Min, RGD peptide cell-surface display enhances the targeting and therapeutic efficacy of attenuated *Salmonella*-mediated cancer therapy, *Theranostics* 6 (2016) 1672–1682, <https://doi.org/10.7150/thno.16135>.

- [22] F. Badie, M. Ghandali, S.A. Tabatabaei, M. Safari, A. Khorshidi, M. Shayestehpour, M. Mahjoubin-Tehran, K. Morshedi, A. Jalili, V. Tajiknia, M.R. Hamblin, H. Mirzaei, Use of *Salmonella* bacteria in cancer therapy: direct, drug delivery and combination approaches, *Front. Oncol.* 11 (2021), 624759, <https://doi.org/10.3389/fonc.2021.624759>.
- [23] J. Chen, Y. Qiao, B. Tang, G. Chen, X. Liu, B. Yang, J. Wei, X. Zhang, X. Cheng, P. Du, W. Jiang, Q. Hu, Z.-C. Hua, Modulation of *Salmonella* tumor-colonization and intratumoral anti-angiogenesis by triptolide and its mechanism, *Theranostics*. 7 (2017) 2250–2260, <https://doi.org/10.7150/thno.18816>.
- [24] L. Jia, D. Wei, Q. Sun, G. Jin, S. Li, Y. Huang, Z. Hua, Tumor-targeting *Salmonella typhimurium* improves cyclophosphamide chemotherapy at maximum tolerated dose and low-dose metronomic regimens in a murine melanoma model, *Int. J. Cancer* 121 (2007) 666–674, <https://doi.org/10.1002/ijc.22688>.
- [25] K. Kawaguchi, K. Miyake, M. Zhao, T. Kiyuna, K. Igarashi, M. Miyake, T. Higuchi, H. Oshiro, M. Bouvet, M. Unno, R.M. Hoffman, Tumor targeting *Salmonella typhimurium* A1-R in combination with gemcitabine (GEM) regresses partially GEM-resistant pancreatic cancer patient-derived orthotopic xenograft (PDOX) nude mouse models, *Cell Cycle* 17 (2018) 2019–2026, <https://doi.org/10.1080/15384101.2018.1480223>.
- [26] C.-H. Lee, C.-L. Wu, A.-L. Shiau, Systemic administration of attenuated *Salmonella choleraesuis* carrying thrombospondin-1 gene leads to tumor-specific transgene expression, delayed tumor growth and prolonged survival in the murine melanoma model, *Cancer Gene Ther.* 12 (2005) 175–184, <https://doi.org/10.1038/sj.cgt.7700777>.
- [27] N.S. Forbes, R.S. Coffin, L. Deng, L. Evgin, S. Fiering, M. Giacalone, C. Gravekamp, J.L. Gulley, H. Gunn, R.M. Hoffman, B. Kaur, K. Liu, H.K. Lyster, A.E. Marciscano, E. Moradian, S. Ruppel, D.A. Saltzman, P.J. Tattersall, S. Thorne, R.G. Vile, H. Zhang, S. Zhou, G. McFadden, White paper on microbial anti-cancer therapy and prevention, *J. Immunoth. Cancer.* 6 (2018) 78, <https://doi.org/10.1186/s40425-018-0381-3>.
- [28] D. Lin, X. Feng, B. Mai, X. Li, F. Wang, J. Liu, X. Liu, K. Zhang, X. Wang, Bacterial-based cancer therapy: an emerging toolbox for targeted drug/gene delivery, *Biomaterials*. 277 (2021), 121124, <https://doi.org/10.1016/j.biomaterials.2021.121124>.
- [29] P.P. Provenzano, C. Cuevas, A.E. Chang, V.K. Goel, D.D.V. Hoff, S.R. Hingorani, Enzymatic targeting of the stroma ablates physical barriers to treatment of pancreatic ductal adenocarcinoma, *Cancer Cell* 21 (2012) 418–429, <https://doi.org/10.1016/j.ccr.2012.01.007>.
- [30] J.-J. Min, H.-J. Kim, J.H. Park, S. Moon, J.H. Jeong, Y.-J. Hong, K.-O. Cho, J. H. Nam, N. Kim, Y.-K. Park, H.-S. Bom, J.H. Rhee, H.E. Choy, Noninvasive real-time imaging of tumors and metastases using tumor-targeting light-emitting *Escherichia coli*, *Mol. Imaging Biol.* 10 (2008) 54–61, <https://doi.org/10.1007/s11307-007-0120-5>.
- [31] R.K. Sironen, M. Tammi, R. Tammi, P.K. Auvinen, M. Anttila, V.-M. Kosma, Hyaluronan in human malignancies, *Exp. Cell Res.* 317 (2011) 383–391, <https://doi.org/10.1016/j.yexcr.2010.11.017>.
- [32] A. Kultti, X. Li, P. Jiang, C.B. Thompson, G.I. Frost, H.M. Shepard, Therapeutic targeting of hyaluronan in the tumor stroma, *Cancers*. 4 (2012) 873–903, <https://doi.org/10.3390/cancers4030873>.
- [33] M. Erkan, S. Hausmann, C.W. Michalski, A.A. Fingerle, M. Dobritz, J. Kleeff, H. Friess, The role of stroma in pancreatic cancer: diagnostic and therapeutic implications, *Nat. Rev. Gastroenterol.* 9 (2012) 454–467, <https://doi.org/10.1038/nrgastro.2012.115>.
- [34] M.A. Jacobetz, D.S. Chan, A. Neesse, T.E. Bapiro, N. Cook, K.K. Frese, C. Feig, T. Nakagawa, M.E. Caldwell, H.I. Zecchini, M.P. Lolkema, P. Jiang, A. Kultti, C. B. Thompson, D.C. Maneval, D.I. Jodrell, G.I. Frost, H.M. Shepard, J.N. Skepper, D. A. Tuveson, Hyaluronan impairs vascular function and drug delivery in a mouse model of pancreatic cancer, *Gut*. 62 (2013) 112–120, <https://doi.org/10.1136/gutjnl-2012-302529>.
- [35] E.A. Turley, P.W. Noble, L.Y.W. Bourguignon, Signaling properties of hyaluronan receptors, *J. Biol. Chem.* 277 (2002) 4589–4592, <https://doi.org/10.1074/jbc.r100038200>.
- [36] C. Chen, S. Zhao, A. Karnad, J.W. Freeman, The biology and role of CD44 in cancer progression: therapeutic implications, *J. Hematol. Oncol.* 11 (2018) 64, <https://doi.org/10.1186/s13045-018-0605-5>.
- [37] T. Garin, A. Rubinstein, N. Grigoriadis, S. Nedvetzki, O. Abramsky, R. Mizrahi-Koll, C. Hand, D. Naor, D. Karussis, CD44 variant DNA vaccination with virtual lymph node ameliorates experimental autoimmune encephalomyelitis through the induction of apoptosis, *J. Neurol. Sci.* 258 (2007) 17–26, <https://doi.org/10.1016/j.jns.2007.01.079>.
- [38] M. Rajasagi, A. von Au, R. Singh, N. Hartmann, M. Zöller, R. Marhaba, Anti-CD44 induces apoptosis in T lymphoma via mitochondrial depolarization, *J. Cell. Mol. Med.* 14 (2010) 1453–1467, <https://doi.org/10.1111/j.1582-4934.2009.00909.x>.
- [39] L. Messina, J.A. Gavira, S. Pernagallo, J.D. Unciti-Broceta, R.M.S. Martin, J.J. Diaz-Mochon, S. Vaccaro, M. Conejero-Muriel, E. Pineda-Molina, S. Caruso, L. Musumeci, R.D. Pasquale, A. Pontillo, F. Sincinelli, M. Pavan, C. Secchieri, Identification and characterization of a bacterial hyaluronidase and its production in recombinant form, *FEBS Lett.* 590 (2016) 2180–2189, <https://doi.org/10.1002/1873-3468.12258>.
- [40] M.E. Hart, M.J. Hart, A.J. Roop, Genotypic and phenotypic assessment of hyaluronidase among type strains of a select group of *Staphylococcal* species, *Int. J. Microbiol.* 2009 (2009), 614371, <https://doi.org/10.1155/2009/614371>.
- [41] S. Uthaman, S. Zheng, J. Han, Y.J. Choi, S. Cho, V.D. Nguyen, J.-O. Park, S.-H. Park, J.-J. Min, S. Park, I.-K. Park, Preparation of engineered *Salmonella typhimurium*-driven hyaluronic-acid-based microbeads with both chemotactic and biological targeting towards breast cancer cells for enhanced anticancer therapy, *Adv. Healthc. Mater.* 5 (2016) 288–295, <https://doi.org/10.1002/adhm.201500556>.
- [42] N.D. Ebelt, K.B. Passi, L.J. Sobocinski, E.R. Manuel, Hyaluronidase-expressing *Salmonella* effectively targets tumor-associated hyaluronic acid in pancreatic ductal adenocarcinoma, *Mol. Cancer Ther.* 19 (2020) 706–716, <https://doi.org/10.1158/1535-7163.MCT-19-0556>.
- [43] X. Liu, Y. Guo, Y. Sun, Y. Chen, W. Tan, J.-J. Min, J.H. Zheng, Comparison of anticancer activities and biosafety between *Salmonella enterica* serovar typhimurium Δ ppGpp and VNP20009 in a murine cancer model, *Front. Microbiol.* 13 (2022), 914575, <https://doi.org/10.3389/fmicb.2022.914575>.
- [44] W. Tan, M.T. Duong, C. Zuo, Y. Qin, Y. Zhang, Y. Guo, Y. Hong, J.H. Zheng, J.-J. Min, Targeting of pancreatic cancer cells and stromal cells using engineered oncolytic *Salmonella typhimurium*, *Mol. Ther.* 30 (2022) 662–671, <https://doi.org/10.1016/j.jymthe.2021.08.023>.
- [45] X. Yi, H. Zhou, Y. Chao, S. Xiong, J. Zhong, Z. Chai, K. Yang, Z. Liu, Bacteria-triggered tumor-specific thrombosis to enable potent photothermal immunotherapy of cancer, *Sci. Adv.* 6 (2020) eaba3546, <https://doi.org/10.1126/sciadv.aba3546>.
- [46] A.M. Farrell, D. Taylor, K.T. Holland, Cloning, nucleotide sequence determination and expression of the *Staphylococcus aureus* hyaluronate lyase gene, *FEMS Microbiol. Lett.* 130 (1995) 81–85, <https://doi.org/10.1111/j.1574-6968.1995.tb07702.x>.
- [47] U.N. Le, H.-S. Kim, J.S. Kwon, M.Y. Kim, V.H. Nguyen, S.-N. Jiang, B.-I. Lee, Y. Hong, M.G. Shin, J.H. Rhee, H.-S. Bom, Y. Ahn, S.S. Gambhir, H.E. Choy, J.-J. Min, Engineering and visualization of bacteria for targeting infarcted myocardium, *Mol. Ther.* 19 (2011) 951–959, <https://doi.org/10.1038/mt.2011.25>.
- [48] A. Dorfman, M.L. Ott, A turbidimetric method for the assay of hyaluronidase, *J. Biol. Chem.* 172 (1948) 367–375.
- [49] U. Ozerdem, A.R. Hargens, A simple method for measuring interstitial fluid pressure in cancer tissues, *Microvasc. Res.* 70 (2005) 116–120, <https://doi.org/10.1016/j.mvr.2005.07.003>.
- [50] P.K. Kim, C.J. Halbrook, S.A. Kerk, M. Radyk, S. Wisner, D.M. Kremer, P. Sajjakulnukit, A. Andren, S.W. Hou, A. Trivedi, G. Thurston, A. Anand, L. Yan, L. Salamanca-Cardona, S.D. Welling, L. Zhang, M.R. Pratt, K.R. Keshari, H. Ying, C. A. Lysiotis, Hyaluronic acid fuels pancreatic cancer cell growth, *Elife*. 10 (2021), e62645, <https://doi.org/10.7554/elif6.62645>.
- [51] K.L. Schwertfeger, M.K. Cowman, P.G. Telmer, E.A. Turley, J.B. McCarthy, Hyaluronan, inflammation, and breast cancer progression, *Front. Immunol.* 6 (2015) 236, <https://doi.org/10.3389/fimmu.2015.00236>.
- [52] T. Chanmee, P. Ontong, N. Itano, Hyaluronan: a modulator of the tumor microenvironment, *Cancer Lett.* 375 (2016) 20–30, <https://doi.org/10.1016/j.canlet.2016.02.031>.
- [53] J. Hyun, S. Jun, H. Lim, H. Cho, S.-H. You, S.-J. Ha, J.-J. Min, D. Bang, Engineered attenuated *Salmonella typhimurium* expressing neoantigen has anticancer effects, *ACS Synth. Biol.* 10 (2021) 2478–2487, <https://doi.org/10.1021/acssynbio.1c00097>.
- [54] S.R. Hingorani, L. Zheng, A.J. Bullock, T.E. Seery, W.P. Harris, D.S. Sigal, F. Braiteh, P.S. Ritch, M.M. Zalupski, N. Bahary, P.E. Oberstein, A. Wang-Gillam, W. Wu, D. Chondros, P. Jiang, S. Khelifa, J. Pu, C. Aldrich, A.E. Hendifar, HALO 202: randomized phase II study of PEGPH20 plus nab-paclitaxel/gemcitabine versus nab-paclitaxel/gemcitabine in patients with untreated, metastatic pancreatic ductal adenocarcinoma, *J. Clin. Oncol.* 36 (2017), <https://doi.org/10.1200/jco.2017.74.9564>.
- [55] F. Petrelli, K. Borgonovo, S. Barni, Targeted delivery for breast cancer therapy: the history of nanoparticle-albumin-bound paclitaxel, *Expert. Opin. Pharmacother.* 11 (2010) 1413–1432, <https://doi.org/10.1517/14656561003796562>.
- [56] A. Benitez, T.J. Yates, L.E. Lopez, W.H. Cerwinka, A. Bakkar, V.B. Lokeshwar, Targeting hyaluronidase for cancer therapy: antitumor activity of sulfated hyaluronic acid in prostate cancer cells, *Cancer Res.* 71 (2011) 4085–4095, <https://doi.org/10.1158/0008-5472.can-10-4610>.